iScience

CellPress
OPEN ACCESS

Article

Systematic analysis of lysine lactylation in nucleus pulposus cells

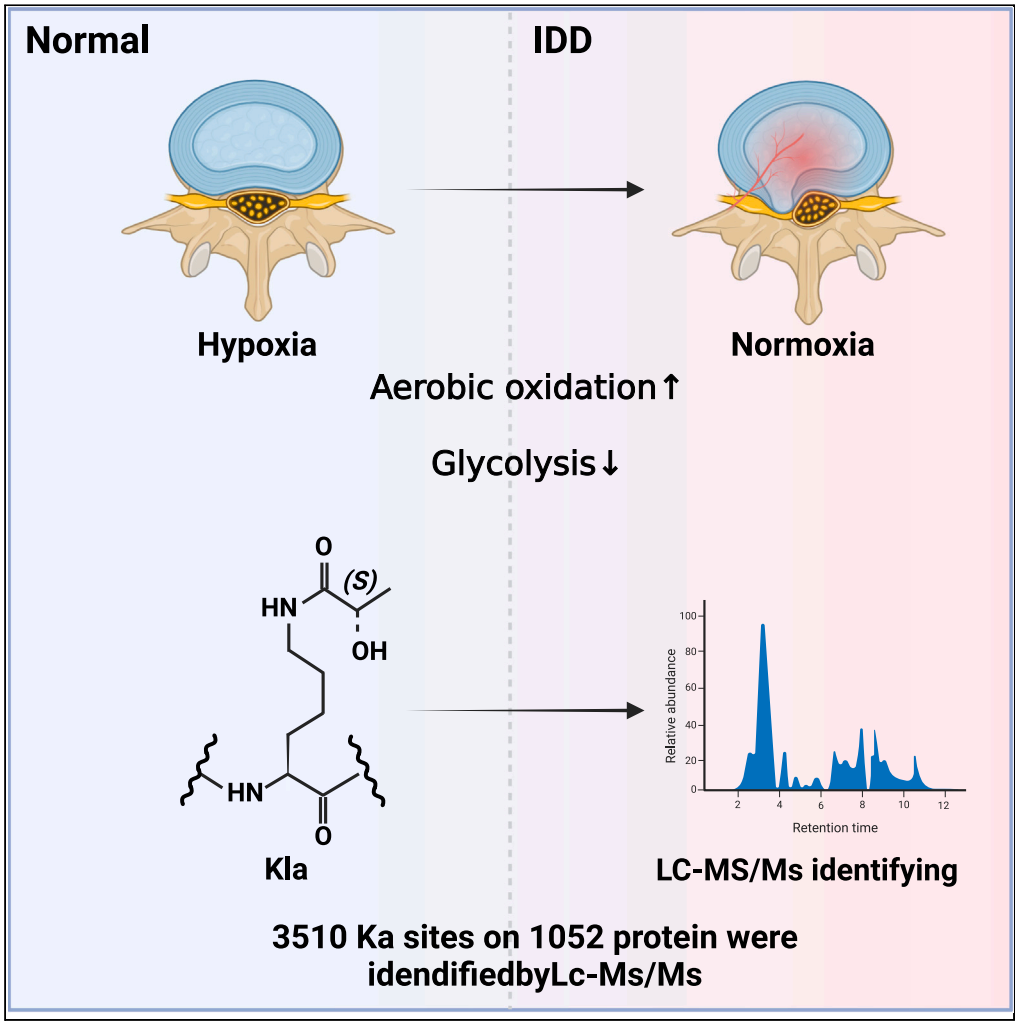

Lei Sheng, Haoran Xu, Yuexing Wang, ..., Xiaozhong Zhou, Kang Wei, Jun Dai

weikang@whu.edu.cn (K.W.)
daijun@suda.edu.cn (J.D.)

Highlights

3510 Kla sites on 1052 non-histone proteins of NPCs cultured in normoxia and hypoxia

Lactylated proteins were significantly enriched in ribosome and spliceosome

Lactate could influence RNA splicing of NPCs

Sheng et al., iScience 27, 111157
November 15, 2024
https://doi.org/10.1016/j.isci.2024.111157

iScience

CellPress
OPEN ACCESS

Article

Systematic analysis of lysine lactylation in nucleus pulposus cells

Lei Sheng,[1,5] Haoran Xu,[3,5] Yuexing Wang,[1,5] Jinhao Ni,[1] Taiyang Xiang,[1] Huanhuan Xu,[4] Xiaozhong Zhou,[1] Kang Wei,[2,*] and Jun Dai[1,6,*]

SUMMARY

Nucleus pulposus (NP) resides in hypoxic microenvironment and NP cells (NPCs), primarily reply on glycolysis and producing high levels of lactate. Intracellular lactate drives lysine lactylation (Kla) as a newly epigenetic modification. However, the impact of Kla on NPCs remains unknown. Here, single-cell RNA sequencing (scRNA-seq) data suggested an altered balance between glycolysis and aerobic oxidation in intervertebral disc degeneration (IDD). Liquid chromatography-tandem mass spectrometry (LC-MS/MS) analysis displayed 3510 lactylation sites on 1052 non-histone proteins of NPCs isolated from rat cultured in normoxia and hypoxia. Moreover, there are 18 proteins with 129 Kla sites and 117 Kla sites in 27 proteins exclusively detected in normoxia and hypoxia group, respectively. Bioinformatics analysis displayed that these lactylated proteins are tightly related to ribosome, spliceosome and the VEGFA-VEGFA2 signaling pathway. Together, our study reveals that Kla may play an important role in regulating cellular metabolism of NPCs.

INTRODUCTION

Intervertebral disc (IVD) as a fibrocartilaginous tissue located in adjacent vertebrae in the spine that absorbs mechanical forces. It consists of jelly-like nucleus pulposus (NP), surrounding annulus fibrosus (AF), and cartilaginous endplate (CEP).[1,2] IVD degeneration (IDD) is an age-related disease and is considered as a major cause of low back pain.[3,4] IDD is involved in multifactorial causes and risk factors including aging, mechanical loading, infection, nutritional factors, and genetic factors.[5] IDD is characterized with extracellular matrix (ECM) degradation, accelerated cartilaginous and bone remodeling, the release of proinflammatory cytokines, altered spine biomechanics, angiogenesis, and neoinnervation, altogether causing low back pain and disability.

Due to complete lack of tissue vascularity, IVD is the largest avascular structure in human body. Consequently, NP resides in a physiologically hypoxic microenvironment, and oxygen levels drop as low as 1%.[6,7] NP cells (NPCs) primarily reply on glycolysis for energy generation and produce lactate which contributes to high lactic acid concentration and relatively low intracellular pH.[8–10] Zhang et al. demonstrated that hypoxia induced production of lactate through glycolysis that in turn served as precursor for stimulating histone lysine lactylation (Kla).[11] Kla as a new post-translational modification directly stimulates gene transcription from chromatin.

Numerous studies revealed histone Kla induced by lactate plays an essential role in regulating metabolic gene expression in tumor cells including NSCLC, HeLa, MCF-7, and HepG2 cells, thereby maintaining tumor survival and growth.[11–13] In addition, some reports uncovered that Kla also occurs on non-histone proteins.[14–16] Lactylation is a vital process linking metabolism and epigenetic modifications that regulate intracellular metabolic disruptions and are involved in various physiological and pathological processes. To date, it remains unclear whether NPCs located in the hypoxic and acidic microenvironment undergo Kla and function of Kla in NPCs. During IDD process, invasion of blood vessels increases the oxygen concentration and consequently alters the physiological hypoxic microenvironment of the IVD[17,18]; and it is unclear whether change of physiological hypoxic microenvironment have impact on Kla.

In this study, we explored the systemic lactylome profiling of NPCs. Single-cell sequencing data was utilized to analyze the metabolic changes in NPCs during IDD and showed that glycolysis was inhibited and aerobic oxidation was enhanced in NPCs during IVD degeneration (IDD). NPCs were cultured under hypoxic and normoxic conditions to mimic the oxygen environments of normal and degenerative NP. We also performed proteomic analysis of NPCs and identified 3510 lactylation sites on 1052 proteins and most of these lactylated proteins were distributed in the nucleus and cytoplasm. In addition, we identified 18 proteins with 129 Kla sites were exclusively detected in the normoxia

[1]Department of Orthopedics, The Second Affiliated Hospital of Soochow University, Suzhou, Jiangsu 215004, China
[2]Department of Plastic Surgery, Zhongnan Hospital of Wuhan University, Wuhan, Hubei 430071, China
[3]Department of Joint Surgery, Center for Orthopedic Surgery, Orthopedic Hospital of Guangdong Province, The Third Affiliated Hospital of Southern Medical University, Guangzhou, Guangdong 510000, China
[4]Department of Obstetrics and Gynecology, Wuhan Children's Hospital, Tongji Medical College, Huazhong University of Science and Technology, Wuhan, Hubei 430000, China
[5]These authors contributed equally
[6]Lead contact
*Correspondence: weikang@whu.edu.cn (K.W.), daijun@suda.edu.cn (J.D.)
https://doi.org/10.1016/j.isci.2024.111157

group, and 117 Kla sites in 27 proteins were specific in hypoxia group. KEGG pathway analysis showed that these proteins were significantly enriched in spliceosome angiogenesis, and ribosome function. Together, the results demonstrated that Kla may play an important role in regulating cellular metabolism.

RESULTS

Single-cell sequencing profiling of human NP tissue

Pyruvate, the end product of glycolysis, is split from glucose.[19] Under hypoxic condition, pyruvate is converted into lactate, whereas it is converted into acetyl-CoA within the mitochondria in normoxic condition. Then acetyl-CoA enters the tricarboxylic acid cycle (TCA cycle) to generate adenosine triphosphate (ATP). To investigate changes of glycometabolism in NPCs during IDD, we analyzed single-cell sequencing data of human NPCs. Based on t-SNE analysis, human NPCs were classified six main clusters including homeostatic NPCs, hypertrophic chondrocyte-like NPCs (HTCL NPCs), fibro NPCs, effector NPCs, adhesion NPCs and regulatory NPCs (Figure 1A). The highly expressed genes of each cluster were shown in Figure 1B. The count and proportion of NPCs changed in IDD group, with decreased proportion of homeostatic and HTCL NPCs and increased proportion of effector and adhesion NPCs (Figures 1C and S1A–S1D). Next, we analyzed trajectory of the NPC subpopulations using CytoTRACE packages and Monocle3. The putative developmental stages of the NPCs differentiation indicated the order of the differentiation states as fibro, adhesion, effector, homeostatic NPCs, regulatory and HTCL NPCs (Figures 1D and 1E). Pseudotime showed that *MMP3*, an ECM degrading marker, was enhanced as NPCs differentiation, indicating the trajectory of NPCs was consistent with the pathological process of IDD (Figure S1E). In addition, lactate metabolism score was decreased with NPCs differentiation (Figure 1F). Gene set variation analysis (GSVA) showed the aerobic oxidation function, such as acetyl-CoA and the TCA cycle were enhanced (Figure 1G). Furthermore, the glucose metabolic functions varied in different subpopulations of NPCs (Figure 1H). For homeostatic and HTCL NPCs, glycolysis function was weakened, and there was no significantly difference in the aerobic oxidation function. In effector and adhesion NPCs glycolysis function was inhibited, and the aerobic oxidation function of glucose was activated (Figure 1H). Taken together, these results indicated that healthy NPCs primarily relied on anaerobic glycolysis for energy metabolism, whereas during IDD the predominant energy-generating pathway was transformed into aerobic oxidation, and the production of lactic acid was reduced. Glycolysis and lactate are closely associated with Kla.[20] Thus, we explore the Kla changes in IDD.

Proteomics analysis and function of NPCs

Given that the glycolysis changes of NPCs in degenerated NP tissues, NPCs were cultured in hypoxia and normoxia environment for 24 h to mimic normal and IDD NP tissues. Before Kla proteome, protein LC-MS/MS and bioinformatics were performed to investigate state of NPCs in hypoxia and normoxia environment (Figure 2A). 4,780 proteins were quantified through the extraction and separation of total proteins (Figure 2B). There were 17 differentially expressed proteins (Figure S2A). Subcellular localization analysis showed 33.47% proteins were distributed in the cytoplasm and 31.96% proteins were located in nucleus (Figure 2C). Furthermore, eight upregulated proteins took part in NOD-like receptor signaling pathway, cell death and gene expression. And nine downregulated proteins participated with necrotic cell death, ferroptosis and cell proliferation. (Figure 2D). Additionally, GSEA analysis showed that the proteins were mainly involved in collagen fibril organization, glycan biosynthesis pathway, encapsulating structure organization and glycoprotein metabolic process which were increased in hypoxia group. And the proteins involved in protein catabolism, glutathione metabolism were upregulated in normoxia group (Figures 2E, 2F, and S2B–S2E). Furthermore, analysis with the HALLMARK database revealed the participation of pathways such as epithelial-mesenchymal transition, hypoxia, and myogenesis (Figures S2F–S2H). To confirm the results of GSEA analysis, NPCs were collected after cultured in hypoxia and normoxia for 24 h. Compared with normoxia conditions, NPCs exhibited higher levels of anabolic index, such as COLLAGEN II, AGGRECAN and SOX9, while the catabolic index MMP3 was decreased in hypoxic condition. (Figures 2G and 2H). Collectively, these findings suggested that NPCs tended to produce more extracellular matrix (ECM) components and fewer MMPs in hypoxic environment, consisting with normal physiological state of NPCs.

Systematic profiling of the Kla proteome in NPCs

Considering that the expression of genes involved in glycolysis and lactate production were decreased and increased levels of TAC and acetyl-CoA pathways in IDD, we explored whether the lactylation level was changed with lactate levels. Kla has been proved in non-histone proteins, but proteome-wide identification of Kla substrates had not been performed in NPCs. To demonstrate proteins bearing Kla in NPCs under normoxia and hypoxia conditions, we carried out proteomic screen through Kla affinity-directed mass spectrometry. Western blotting analysis confirmed that Kla level was higher in NPCs under hypoxia conditions (Figures 3A and S3A). Brilliant Blue staining showed that multiple protein bands with different molecular weights were detected, indicating the presence of Kla in non-histone proteins (Figure 3B). To characterize the global Kla of proteins in NPCs, whole-cell extractions were subjected to LC-MS/MS analysis (Figure 3C). The mass validation of large-scale data conformed to the following criteria: mass error $\leq$5 ppm and localization probability >75% (Figure S3B). Moreover, the length distribution of NPCs peptides detected met quality standards (most of the peptides were distributed in 7–20 amino acids) (Figure S3C). Most of lactylated proteins in NPCs were distributed in the nucleus (39.06%) and cytoplasm (37.34%) (Figure 3D). The proportion of subcellular structural Kla proteins altered in response to changes in the oxygen environment (Figure 3D). LC-MS/MS quantified 3,510 Kla sites in 1,052 proteins, and 129 Kla sites in 18 proteins and 27 proteins with 117 Kla sites were exclusive in normoxia and hypoxia group, respectively (Figure 3E). 75.29% lactylated proteins had 1-3 Kla sites, and 12.36% proteins had more than 5 Kla sites (Figures 3F and S3D).

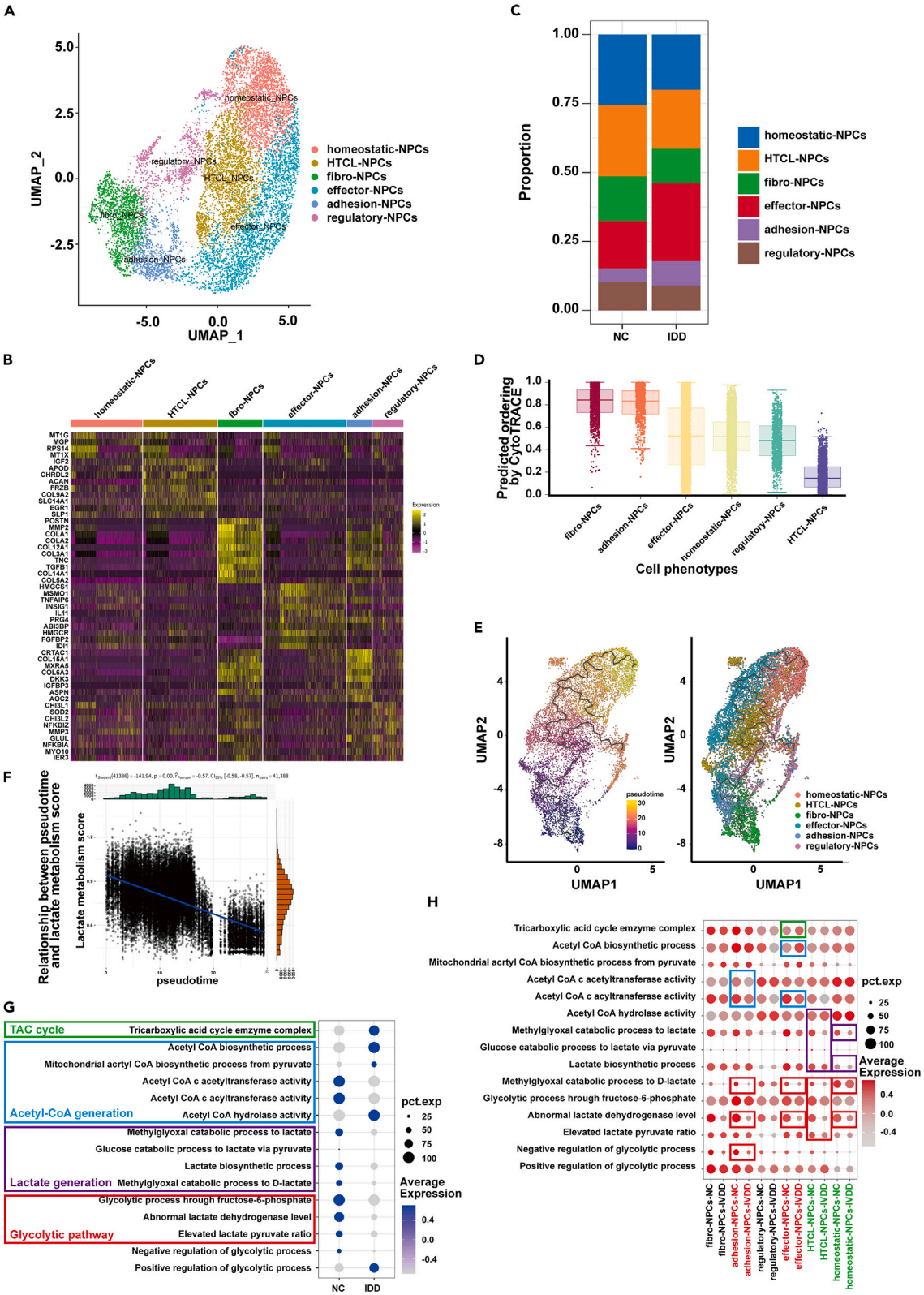
A
UMAP_2
UMAP_1
homeostatic_NPCs
HTCL-NPCs
fibro-NPCs
effector-NPCs
adhesion-NPCs
regulatory-NPCs
B
homeostatic-NPCs
HTCL-NPCs
fibro-NPCs
effector-NPCs
adhesion-NPCs
regulatory-NPCs
Expression
C
Proportion
NC
IDD
D
Predicted ordering by CytoTRACE
Cell phenotypes
E
UMAP2
UMAP1
pseudotime
F
Relationship between pseudotime and lactate metabolism score
Lactate metabolism score
pseudotime
G
TAC cycle
Tricarboxylic acid cycle emzyme complex
Acetyl CoA biosynthetic process
Mitochondrial acrtyl CoA biosynthetic process from pyruvate
Acetyl CoA c acetyltransferase activity
Acetyl CoA c acyltransferase activity
Acetyl-CoA generation
Acetyl CoA hydrolase activity
Methylglyoxal catabolic process to lactate
Glucose catabolic process to lactate via pyruvate
Lactate biosynthetic process
Lactate generation
Methylglyoxal catabolic process to D-lactate
Glycolytic process hrough fructose-6-phosphate
Abnormal lactate dehydrogenase level
Elevated lactate pyruvate ratio
Glycolytic pathway
Negative regulation of glycolytic process
Positive regulation of glycolytic process
pct.exp
Average Expression
NC
IDD
H
Tricarboxylic acid cycle emzyme complex
Acetyl CoA biosynthetic process
Mitochondrial acrtyl CoA biosynthetic process from pyruvate
Acetyl CoA c acetyltransferase activity
Acetyl CoA c acyltransferase activity
Acetyl CoA hydrolase activity
Methylglyoxal catabolic process to lactate
Glucose catabolic process to lactate via pyruvate
Lactate biosynthetic process
Methylglyoxal catabolic process to D-lactate
Glycolytic process hrough fructose-6-phosphate
Abnormal lactate dehydrogenase level
Elevated lactate pyruvate ratio
Negative regulation of glycolytic process
Positive regulation of glycolytic process
pct.exp
Average Expression
fibro-NPCs-NC
fibro-NPCs-iVDD
adhesion-NPCs-NC
adhesion-NPCs-iVDD
regulatory-NPCs-NC
regulatory-NPCs-iVDD
effector-NPCs-NC
effector-NPCs-iVDD
HTCL-NPCs-NC
HTCL-NPCs-iVDD
homeostatic-NPCs-NC
homeostatic-NPCs-iVDD

Figure 1. Single-cell atlas of degenerated NP tissues and metabolic changes during IDD

(A) T-Distributed Stochastic Neighbor Embedding (tSNE) visualization of human NPCs identifying six clusters after unsupervised clustering

(B) Heatmap of typically expressed genes in each cell cluster.

(C) The proportion of NPCs in NC and IDD of human NP tissues.

(D) CytoTRACE analysis of predicted ordering for NPCs.

(E) Pseudotime analysis of the six NPCs subclusters.

(F) The lactate metabolism score decreases with pseudotime.

(G) GSVA analysis showing the changes of glucose metabolism during IDD.

(H) Variations in glucose metabolism across different NPCs subclusters.

MoMo software tool was employed to analyze the amino acid sequence surrounding the Kla sites in all identified peptides, spanning from −10 to +10 positions. According to the enrichment statistics, we identified several conserved motifs, such as xxxKxxxxxx_K_MPxxxxxxxx, xxxPxxxxxx_K_xxxxKxxxDx, and xxxxxxxxxx_K_xxxxxxKMPx. In these sites, lysine (K) and proline (P) residues were identified as the most frequent residues in each lactylation motif (Figure 4A and Data S1). The number of instances of each conserved motif in the NPCs sample was shown in Figure 4B. Heatmaps of the amino acid sequences surrounding lactylation sites demonstrated that lysine (K) residues were enriched in the regions from −10 to −3 and from +5 to +10, and Alanine (A) residues were enriched in the regions from −8 to −1 and from +1 to +7 positions (Figure 4C). Previous studies reported the possible Kla motifs, whereas results of Kla motif in NPCs differ from those identified in gastric cancer cells, Phialophora verrucosa, *Oryza sativa*, and *Botrytis cinerea*.[14,16,21,22] Representative MS/MS spectra of three lactylated proteins including PSMD6, PKM and FTH are shown in Figures 4D–4F.

Functional enrichment analysis of lactylated proteins in NPCs

To investigate the function of lactylated proteins in normoxia or hypoxia groups, we performed analysis of Gene Ontology (GO) functional annotations and found that lactylated proteins were involved in RNA splicing and processing (Figure 5A). Kyoto Encyclopedia of Genes and Genomes (KEGG) analysis showed that proteins related to the spliceosome, necroptosis, glycolysis/gluconeogenesis (Table S1) and carbon metabolism were more likely to be lactylated (Figure 5B). In hypoxia group, proteins with high lactylation level were involved in RNA splicing, including splicing factor 3a, subunit 1 (SF3A1), pre-mRNA-splicing factor 3 (PRPF3), pre-mRNA-splicing factor 6 (PRPF6) and pre-mRNA-splicing factor 31(PRPF31) (Figures 5C and 5E, Table S2), suggesting that Kla affected RNA splicing. However, the lactylated proteins in normoxia group were related with ribosome and participated in ribonucleoprotein complex biogenesis and actin binding (Figures 5D and 5F, Table S3). These results suggested that proteins with Kla sites exclusively in hypoxia and normoxia group were closely associated with the regulation of RNA splicing and ribonucleoprotein complex biogenesis.

In addition, 39 proteins with differential levels of lactylation were involved in gene transcription and expression functions, and were also associated with various molecular functions, such as ADP/ATP binding, histone deacetylase activity, ubiquitin protein ligase activity, hydrolase activity and pyrophosphatase activity (Figures S4A–S4C). The biological processes of these proteins were involved in protein localization to cell surface, mitochondrial membrane organization and cellular oxidant detoxification (Figure S4D). Overall, these findings indicated the lactylation of NPC proteins appears to undergo transformations in response to changes in the microenvironment.

Protein-protein interaction (PPI) network of lactylated proteins in NPCs

To further understand the cellular processes regulated by lactylated proteins in NPCs, PPI network was constructed using Cytoscape software. A total of 1,041 lactylated proteins, comprising 3,470 Kla sites, were mapped to the database using the STRING database (confidence score >0.9). The blue and red fill represented lysine sites lactated in the normoxia and hypoxia group, and the green fill indicated lactated amino acid sites in both normoxia and hypoxia groups. Additionally, red circles denoted a high level of lactylation in hypoxia group, and green circles indicated a high level of lactylation in normoxia group. Using PPI network, five important modules were identified including Module 1 (ribosomal protein family), Module 2 (proteasome complex), Module 3 (eukaryotic translation initiation factor family), Module 4 (T-complex protein family), and Module 5 (heterogeneous nuclear ribonucleoprotein family) (Figure 6A). The functions of five modules were determined by analyzing the Hallmark, GO-BP, KEGG and WIKI databases. As showed in Figure 6B, module 1 was associated with cytoplasmic translation, ribonucleoprotein complex biogenesis, VEGFA-VEGFR2 signaling pathway, ubiquitin ligase inhibitor activity and mRNA binding. Module 2 was related to mRNA binding, cadherin binding, and eukaryotic translation initiation factor 2 complex. Module 3 and Module 4 were involved with regulation of RNA splicing and mRNA binding and transcription factor binding and proteasome, respectively. Module 5 was affiliated with positive regulation of establishment of protein localization to telomere (Figure 6B). During IDD, invasion of blood vessels increases the oxygen concentration and consequently alters the physiological hypoxic microenvironment of IVD.[23,24] Western blotting analysis showed that VEGFA level decreased in NPCs under hypoxia environment and endothelial progenitor cells (EPCs) treated with conditioned medium from normoxic NPCs exhibited the activation of angiogenesis (Figures 6C and 6D). Therefore, these results demonstrated that lactylation potentially altered the associated biological processes, such as angiogenesis in NPCs.

DISCUSSION

IVD is the largest avascular structure in human body and NPCs primarily reply on glycolysis for energy generation and produce lactate which contributes to high lactic acid environment in healthy NP tissue. Intracellular lactate can result in a newly epigenetic modification-lysine

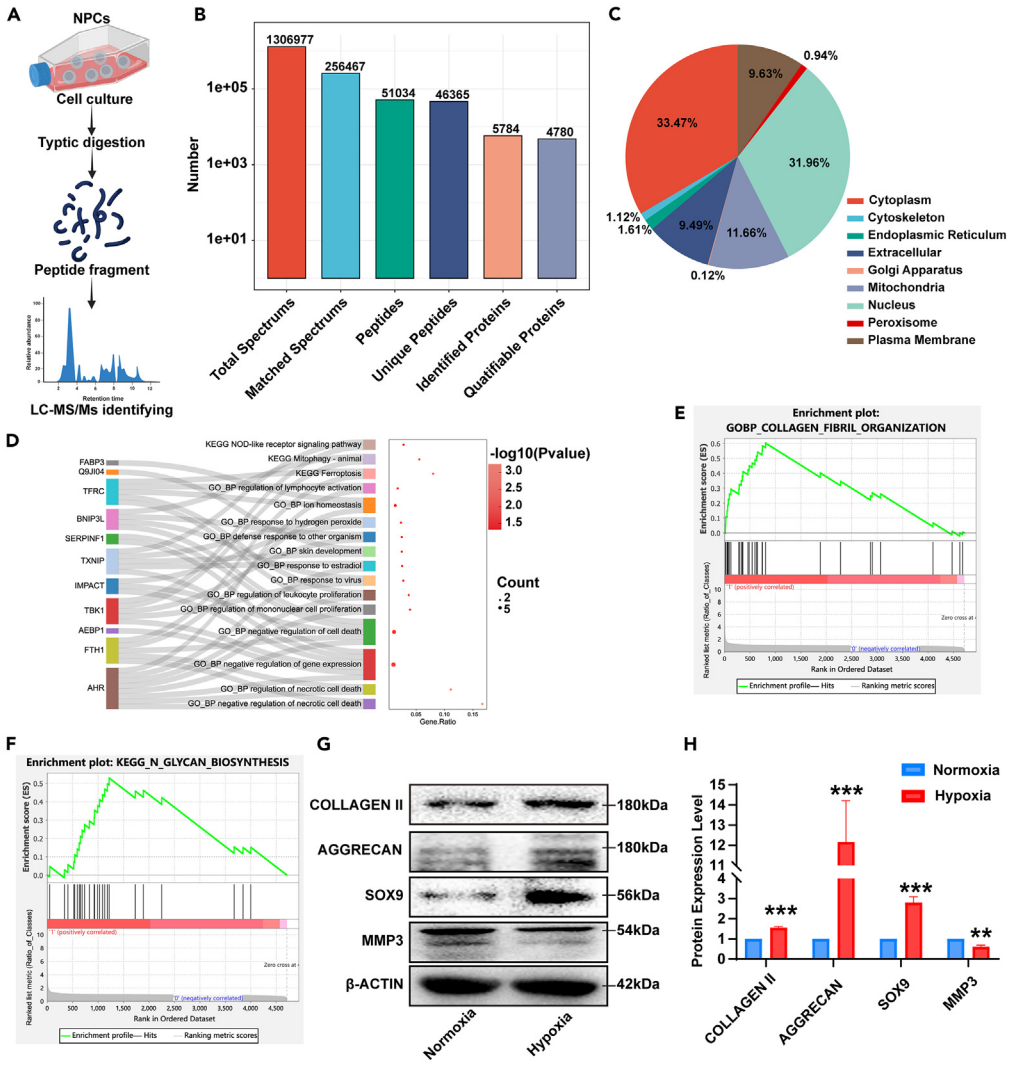

Figure 2. Proteomics analysis of NPCs under normoxia and hypoxia conditions

(A) A schematic flow chart for protein LC-MS/MS in NPCs.

(B) LC-MS/MS data depicting the proteomic profile of NPCs in normoxia and hypoxia groups. Total spectrums: the number of secondary spectrums generated by mass spectrometry; Matched spectrums: the number of spectrums that match theoretical secondary spectrums; Peptides: the number of peptide sequences identified from the matching results; Unique peptides: the number of unique peptide sequences identified from the matching results; Identified proteins: the number of proteins identified through specific peptide sequences; Quantifiable proteins: the number of proteins quantified through specific peptide sequences.

(C) The subcellular distribution of different Kla level protein in NPCs.

(D) Visualization of the functional role of proteins in NPCs based on GO or KEGG analysis.

(E and F) GSEA analysis of collagen fibril organization and glycan biosynthesis in hypoxia NPCs.

(G) Western blotting analysis of anabolism related proteins including COLLAGEN II, AGGRECAN, MMP3 and SOX9 in NPCs, and (H) its quantification, (n = 3 biological replicates per group). Data are represented as mean ± SEM, and the p value was calculated by an unpaired two-tailed Student's t test.

lactylation (Kla). However, the impact of Kla on NPCs remains obscure. In this study, single-cell sequencing of human NPCs analysis revealed that during IDD predominant energy-generating pathway was transformed into aerobic oxidation, and the production of lactic acid was reduced. Then we identified 3,510 Kla sites in 1,052 proteins in NPCs, and found that 129 Kla sites in 18 proteins and 27 proteins with 117 Kla sites were exclusive in normoxia and hypoxia group, respectively. Furthermore, bioinformatics analysis suggested that proteins with Kla sites exclusively in hypoxia and normoxia group were closely associated with the regulation of RNA splicing and ribonucleoprotein complex biogenesis. Taken together, these data revealed that that Kla plays an important role in regulating cellular metabolism in NPCs and participated in RNA splicing and ribonucleoprotein complex biogenesis.

Kla is mainly characterized on the histones which plays an important role in regulating gene expression in tumorigenesis,[20,25] inflammation,[26,27] and regeneration.[28] Recently, a set of studies revealed that Kla also occurs on non-histone proteins and systemic analysis of Kla in

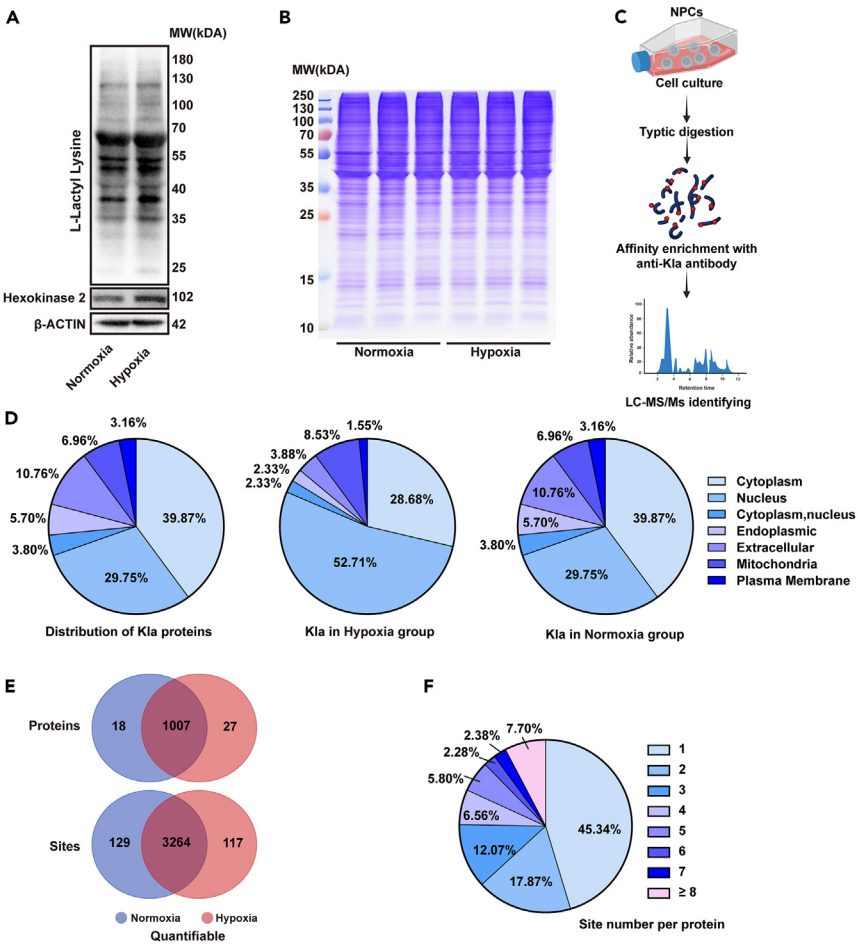

Figure 3. Systematic profiling of the Kla proteome in NPCs

(A) Western blotting analysis of lactylation and hexokinase 2 levels in NPCs.

(B) Coomassie brilliant blue staining of SDS-PAGE samples for mass spectrometry.

(C) A schematic flow chart for identification of Kla-containing protein substrates in NPCs.

(D) The subcellular distribution of Kla proteins.

(E) Venn diagrams of identified or quantifiable lactylated proteins and amino acid sites in normoxia and hypoxia NPCs.

(F) Pie chart showing the distribution of the total number of lactylated sites per protein.

plant fungal pathogen botrytis cinerea,[14] polymicrobial sepsis[15] and gastric cancer cells[16] have been explored. Due to complete lack of tissue vascularity in IVD, NP resides in a physiologically hypoxic microenvironment, and oxygen levels is as low as 1%.[6,7] NPCs primarily reply on glycolysis for energy generation and result in high lactic acid concentration.[8–10] During IDD, the lactate metabolism was inhibited, whereas the aerobic oxidation was enhanced which is consistent with prior studies.[6,7,29–31] Therefore, we established an atlas of non-histone Kla proteins in NPCs, which comprised a total of 1,052 proteins with 3,510 lysine sites. Importantly, we identified 18 proteins with 129 lactylated sites in normoxic condition, and 27 proteins with 117 lactylated sites exclusively in hypoxic environment. Wang et al. uncovered that hypoxia increased lactylation in microglia and identified 77 sites of lactylated 67 proteins with increased in the context of increased lactate under hypoxia.[32] It is noteworthy that lactic acid plays a significant role not only in anoxic NPCs but also in normoxic conditions. However, the specific amino acid sites of lactylated proteins differed in response to changes in oxygen availability.

The lactylated proteins were enriched in spliceosome functions, suggesting a global influence of lactate on RNA splicing. RNA splicing plays a crucial role in the regulation of gene expression and are essential for multiple cellular progress.[33–37] The spliceosome removes introns from pre-mRNA, allowing the exons to join together and generate mature mRNA. Yang et al. revealed that Kla proteins were enriched in spliceosome functions in gastric cancer cells including SF3B1 and hnRNPA1, which regulate alternative splicing.[16] In addition, Lactylated proteins were also closely related to mRNA splicing in *Toxoplasma gondii*, participating in precisely controlling gene expression.[38] Similarly, we found that the spliceosome-related lactylated proteins such as pre-mRNA processing factor (PRPF) family and splicing factor 3 (SF3). The ribosome, composed of RNA and protein, is responsible for the translation of mRNA into functional proteins in all biological systems.[39] In our study, 23 lactylated proteins were associated with the ribosome in normoxia group. While

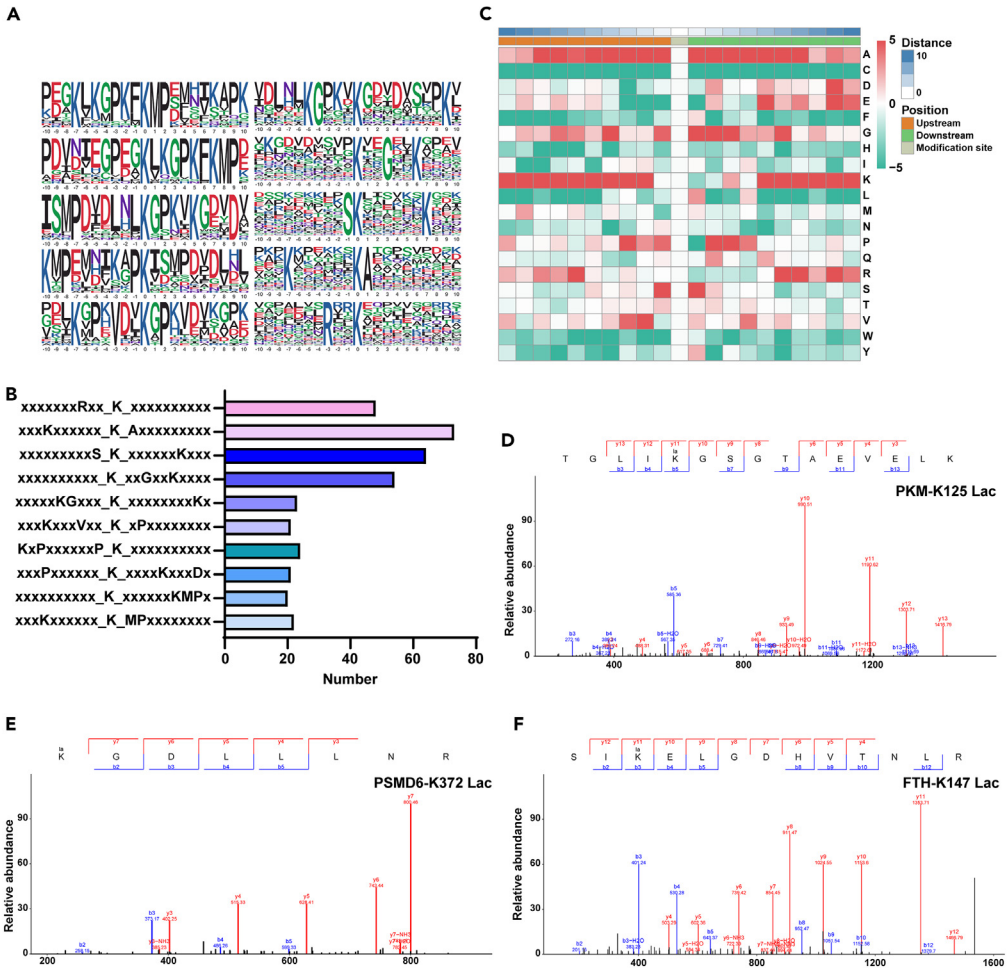

Figure 4. Properties of Kla peptides

(A) Lactylation sequence motifs for ±10 amino acids surrounding the Kla sites with Motif-X software. The central K (at position indicates the lactylation lysine. All the surrounding amino acid residues are indicated with the letters in different sizes which is consistent with their frequencies in respective positions. Alanine (A), arginine (R), aspartic acid (D), cysteine (C), glutamine (Q), glutamic acid (E), histidine (H), isoleucine (I), glycine (G), asparagine (N), leucine (L), lysine (K), methionine (M), phenylalanine (F), proline (P), serine (S), threonine (T), tryptophan (W), tyrosine (Y), valine (V).

(B) The number of instances of each conserved motif in NPCs.

(C) Heatmap of the amino acid compositions of the Kla sites demonstrating the frequency of certain amino acids around the modified lysine. Red indicates high frequency and green means low frequency.

(D–F) Tandem mass spectroscopy (MS/MS) spectra of three representative Kla peptides from PKM, PSMD6, and FTH.

phosphorylation, acetylation, and methylation are well-known protein modifications associated with ribosomes, this study discovers lactylated proteins in NPCs' ribosomes. In higher eukaryotes, most genes are transcribed as pre-mRNAs, which contain both exons and intervening introns.[40] The ribosome, composed of RNA and protein, facilitates the conversion of mRNA into functional proteins across all biological systems.[39] Taken together, lactylated proteins shown in our study may likely provide insights into the regulation of gene transcription and expression.

We utilized the MCODE plugin to investigate five crucial modules in the protein-protein interaction (PPI) network. Module 1 was found to inhibit the activity of ubiquitinated ligase. This is particularly significant in the context of intervertebral disc degeneration (IDD), as protein ubiquitination plays a regulatory role in the senescence, apoptosis, and inflammation of NPCs.[41,42] Ubiquitinated proteins are typically transported to the lysosome or proteasome for degradation.[43] Notably, module 4 was found to regulate the proteasome. Moreover, module 1 was also found to impact the VEGFA-VEGFR2 signaling pathway. Vascularization of the intervertebral disc (IVD) has long been recognized as a pathological feature of IDD.[44] Interestingly, western blot analysis revealed a high level of VEGFA, indicating that the hypoxic microenvironment inhibits angiogenesis. Additionally, modules 1, 2, and 3 were found to be involved in mRNA binding. These findings shed light on the intricate molecular mechanisms underlying IDD and provide valuable insights into the regulation of senescence, apoptosis, inflammation, proteasome activity, angiogenesis, and mRNA binding processes.

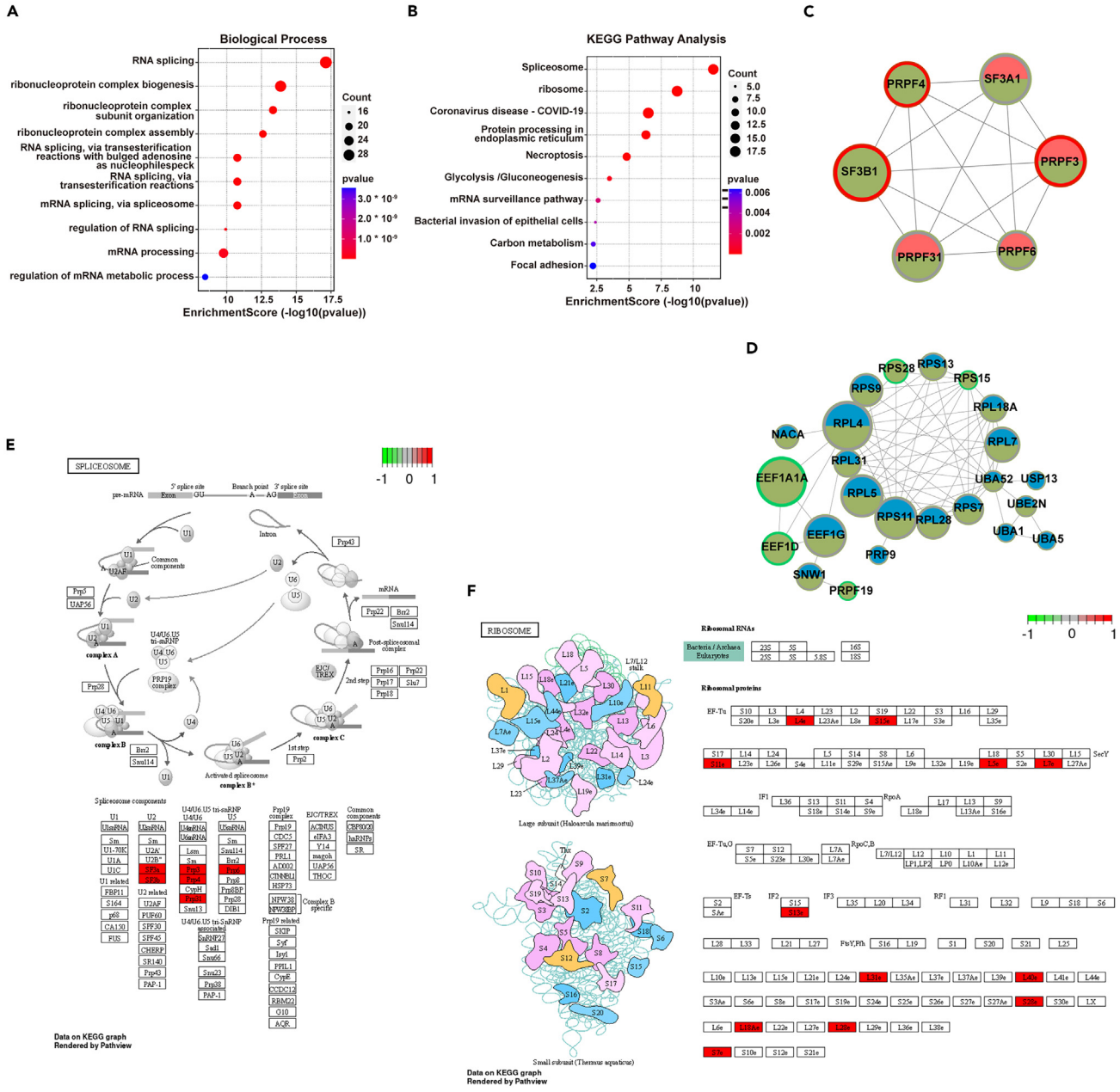

Figure 5. Functional analysis of proteins with Kla sites exclusive in normoxia and hypoxia groups

(A) GO-based enrichment analysis of Kla proteins.

(B) KEGG pathway-based enrichment analysis of modified proteins.

(C and D) PPI network of Kla protein or Kla sites exclusively in the hypoxia and normoxia group.

(E and F) Wiring diagrams of the Kla proteins enriched in the spliceosome and ribosome pathway of hypoxia and normoxia groups.

Furthermore, our study revealed the presence of lactylated enzymes involved in glucose metabolism, such as ALDOA, AKR1A1, PDHA1, TPI1, GPI, and PKM. We identified changes in lactylation at specific sites on these enzymes. For example, GPI showed alterations at lactylation sites K25 and K73, while Tpi1 exhibited changes at K59 and K142 lactylation sites. Akr1a1 displayed modifications at lactylation sites K153 and K127. Aldoa and Pdha1 had alterations at lactylation sites K13 and K63, respectively. Pyruvate kinase (PK), a key enzyme in glycolysis, exists in four distinct subtypes: L, R, M1, and M2.[45] PKM2 is found in tissues such as the brain and liver, while PKM1 is located in the myocardium, skeletal muscle, and brain tissue.[46] PK catalyzes the conversion of phosphoenolpyruvate (PEP) to pyruvate.[47] Intriguingly, we identified five lactylation site changes (K3, K25, K207, K305, and K322) on PKM. These lactylation alterations may play a crucial role in regulating pyruvate levels,

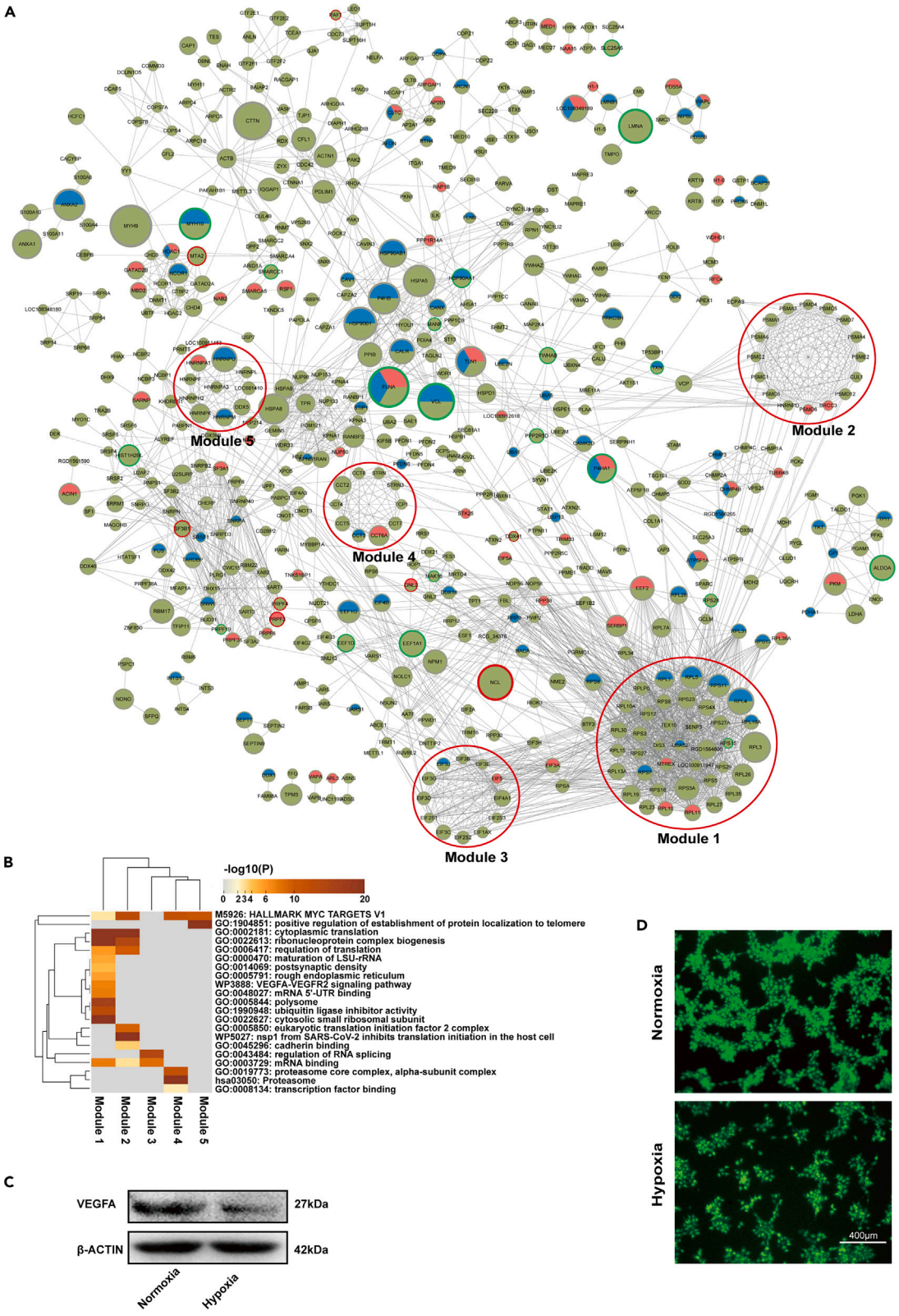
A
Module 1
Module 2
Module 3
Module 4
Module 5
B
-log10(P)
0 2 3 4 6 10 20
M5926: HALLMARK MYC TARGETS V1
GO:1904851: positive regulation of establishment of protein localization to telomere
GO:0002181: cytoplasmic translation
GO:0022613: ribonucleoprotein complex biogenesis
GO:0006417: regulation of translation
GO:0000470: maturation of LSU-rRNA
GO:0014069: postsynaptic density
GO:0005791: rough endoplasmic reticulum
WP3888: VEGFA-VEGFR2 signaling pathway
GO:0048027: mRNA 5'-UTR binding
GO:0005844: polysome
GO:1990948: ubiquitin ligase inhibitor activity
GO:0022627: cytosolic small ribosomal subunit
GO:0005850: eukaryotic translation initiation factor 2 complex
WP5027: nsp1 from SARS-CoV-2 inhibits translation initiation in the host cell
GO:0045296: cadherin binding
GO:0043484: regulation of RNA splicing
GO:0003729: mRNA binding
GO:0019773: proteasome core complex, alpha-subunit complex
hsa03050: Proteasome
GO:0008134: transcription factor binding
Module 1
Module 2
Module 3
Module 4
Module 5
C
VEGFA
27kDa
β-ACTIN
42kDa
Normoxia
Hypoxia
D
Normoxia
Hypoxia
400μm

Figure 6. The top five clusters of highly interconnected lactylated protein networks in NPCs

(A) PPI networks of Kla proteins in NPCs with Mcode tool. Blue filling: The presence of a modification site on this protein only occurs in the NC group; Red filling: The presence of a modification site on this protein only occurs in the HY group; Green filling: The modification sites on the protein were lactated in both NC and HY groups; Red surround: HY/NC up-regulated modification site exists in this protein; Green surround: there are NC/HY up-regulation modification sites in this protein.

(B) KEGG pathway analysis of five modules from (A).

(C) Western blotting analysis of VEGFA in NPCs.

(D) IF staining of EPC tube formation with Calcein-AM. The scale bar is 400 μm.

which are vital for cellular processes. However, further research is necessary to fully understand the biological significance of these lactylation modifications.

Our data strongly suggest that the metabolic shift of NPCs from aerobic to anaerobic metabolism during IDD, and the corresponding transformation of protein lactylation in response to microenvironment changes. The transformation of protein lactylation influences vascularization of the IVD, as well as the function of the spliceosome and ribosome. The data provides insights into the functional consequences of amino acid site-specific protein lactylation during IDD, particularly in the context of pathological normoxic conditions, and may pave the way for elucidating the mechanisms underlying IDD.

Limitations of the study

We proposed that the metabolic status of NPCs undergoes changes in response to the altered oxygen environment within the IVD, leading to variations in protein lactylation. This acute microenvironment change may not consistent with the gradually and chronic condition of IDD progression, and the final lactylation pattern of proteins may be different between the acute *in vitro*, and the gradual chronic *in vivo* condition. And the functional significance of lactylated proteins was analyzed using bioinformatics. To address this, our ongoing laboratory investigations aim to validate the biological functions of lactylated proteins.

RESOURCE AVAILABILITY

Lead contact

Further information and requests for resources and reagents should be directed to and will be fulfilled by the lead contact, Jun Dai (daijun@suda.edu.cn).

Materials availability

This study did not generate new unique reagents.

Data and code availability

- The mass spectrometry proteomics data has been deposited to the ProteomeXchange Consortium via the PRIDE partner repository. The accession number is listed in the key resources table. They are available upon request if access is granted.
- This paper does not report original code.
- Any additional information required to reanalyze the data reported in this paper is available from the lead contact upon request.

ACKNOWLEDGMENTS

This study was sponsored by the National Natural Science Foundation of China (82002345, 81902179), the Natural Science Foundation of Jiangsu Province (BK20221241), the Science and Technology Project of Suzhou (KJXW2019011), Gusu Health Personnel Scientific Research Project (Qngg2022008), the Gusu Talent Program (GSWS2021027 and GSWS2022046), the Preliminary Research Project of the Second Affiliated Hospital of Soochow University (SDFEYBS1905) and the Postdoctoral Fellowship Program of China Postdoctoral Science Foundation (GZC20241275).

AUTHOR CONTRIBUTIONS

L.S.: Funding acquisition, Visualization and Writing–review and editing. **H.X.:** Methodology and Investigation. **Y.W.:** Data curation. **J.N.:** Data curation. **T.X.:** Software. **H.X.:** Software. **X.Z.:** Visualization. **K.W.:** Funding acquisition, Supervision and visualization. **J.D.:** Funding acquisition and project administration.

DECLARATION OF INTERESTS

The authors declare that they have no conflicts of interest.

STAR★METHODS

Detailed methods are provided in the online version of this paper and include the following:

- KEY RESOURCES TABLE
- EXPERIMENTAL MODEL AND STUDY PARTICIPANT DETAILS
  - Cell culture
- METHOD DETAILS
  - Single-cell data analysis
  - Western blotting analysis
  - Proteomic analysis

SUPPLEMENTAL INFORMATION

Supplemental information can be found online at https://doi.org/10.1016/j.isci.2024.111157.

Received: December 13, 2023
Revised: May 28, 2024
Accepted: October 9, 2024
Published: October 11, 2024

REFERENCES

1. Dowdell, J., Erwin, M., Choma, T., Vaccaro, A., Iatridis, J., and Cho, S.K. (2017). Intervertebral Disk Degeneration and Repair. Neurosurgery *80*, S46–S54. https://doi.org/10.1093/neuros/nyw078.
2. Gradišnik, L., Maver, U., Gole, B., Bunc, G., Voršič, M., Ravnik, J., Amigoc, T., Bošnjak, R., and Velnar, T. (2022). The Endplate Role in Degenerative Disc Disease Research: the Isolation of Human Chondrocytes from Vertebral Endplate-an Optimised Protocol. Bioengineering *9*, 137. https://doi.org/10.3390/bioengineering9040137.
3. Knezevic, N.N., Candido, K.D., Vlaeyen, J.W.S., Van Zundert, J., and Cohen, S.P. (2021). Low back pain. Lancet (London, England) *398*, 78–92. https://doi.org/10.1016/S0140-6736(21)00733-9.
4. Zheng, C.J., and Chen, J. (2015). Disc degeneration implies low back pain. Theor. Biol. Med. Model. *12*, 24. https://doi.org/10.1186/s12976-015-0020-3.
5. Meisel, H.J., Agarwal, N., Hsieh, P.C., Skelly, A., Park, J.B., Brodke, D., Wang, J.C., Yoon, S.T., and Buser, Z. (2019). Cell Therapy for Treatment of Intervertebral Disc Degeneration: a Systematic Review. Glob. Spine J. *9*, 39S–52S. https://doi.org/10.1177/2192568219829024.
6. Buckley, C.T., Hoyland, J.A., Fujii, K., Pandit, A., Iatridis, J.C., and Grad, S. (2018). Critical aspects and challenges for intervertebral disc repair and regeneration-Harnessing advances in tissue engineering. JOR Spine *1*, e1029. https://doi.org/10.1002/jsp2.1029.
7. Guerrero, J., Häckel, S., Croft, A.S., Hoppe, S., Albers, C.E., and Gantenbein, B. (2021). The nucleus pulposus microenvironment in the intervertebral disc: the fountain of youth? Eur. Cells Mater. *41*, 707–738. https://doi.org/10.22203/eCM.v041a46.
8. Urban, J.P.G., Smith, S., and Fairbank, J.C.T. (2004). Nutrition of the intervertebral disc. SPINE *29*, 2700–2709. https://doi.org/10.1097/01.brs.0000146499.97948.52.
9. Madhu, V., Boneski, P.K., Silagi, E., Qiu, Y., Kurland, I., Guntur, A.R., Shapiro, I.M., and Risbud, M.V. (2020). Hypoxic Regulation of Mitochondrial Metabolism and Mitophagy in Nucleus Pulposus Cells is Dependent on HIF-1α-BNIP3 Axis. J. Bone Miner. Res. *35*, 1504–1524. https://doi.org/10.1002/jbmr.4019.
10. Silagi, E.S., Schoepflin, Z.R., Seifert, E.L., Merceron, C., Schipani, E., Shapiro, I.M., and Risbud, M.V. (2018). Bicarbonate Recycling by HIF-1-Dependent Carbonic Anhydrase Isoforms 9 and 12 is Critical in Maintaining Intracellular pH and Viability of Nucleus Pulposus Cells. J. Bone Miner. Res. *33*, 338–355. https://doi.org/10.1002/jbmr.3293.
11. Zhang, D., Tang, Z., Huang, H., Zhou, G., Cui, C., Weng, Y., Liu, W., Kim, S., Lee, S., Perez-Neut, M., et al. (2019). Metabolic regulation of gene expression by histone lactylation. Nature *574*, 575–580. https://doi.org/10.1038/s41586-019-1678-1.
12. Jiang, J., Huang, D., Jiang, Y., Hou, J., Tian, M., Li, J., Sun, L., Zhang, Y., Zhang, T., Li, Z., et al. (2021). Lactate Modulates Cellular Metabolism through Histone Lactylation-Mediated Gene Expression in Non-Small Cell Lung Cancer. Front. Oncol. *11*, 647559. https://doi.org/10.3389/fonc.2021.647559.
13. Smith, E.A., and Hodges, H.C. (2019). The Spatial and Genomic Hierarchy of Tumor Ecosystems Revealed by Single-Cell Technologies. Trends Cancer *5*, 411–425. https://doi.org/10.1016/j.trecan.2019.05.009.
14. Gao, M., Zhang, N., and Liang, W. (2020). Systematic Analysis of Lysine Lactylation in the Plant Fungal Pathogen Botrytis cinerea. Front. Microbiol. *11*, 594743. https://doi.org/10.3389/fmicb.2020.594743.
15. Yang, K., Fan, M., Wang, X., Xu, J., Wang, Y., Tu, F., Gill, P.S., Ha, T., Liu, L., Williams, D.L., and Li, C. (2022). Lactate promotes macrophage HMGB1 lactylation, acetylation, and exosomal release in polymicrobial sepsis. Cell Death Differ. *29*, 133–146. https://doi.org/10.1038/s41418-021-00841-9.
16. Yang, D., Yin, J., Shan, L., Yi, X., Zhang, W., and Ding, Y. (2022). Identification of lysine-lactylated substrates in gastric cancer cells. iScience *25*, 104630. https://doi.org/10.1016/j.isci.2022.104630.
17. Freemont, A.J., Watkins, A., Le Maitre, C., Baird, P., Jeziorska, M., Knight, M.T.N., Ross, E.R.S., O'Brien, J.P., and Hoyland, J.A. (2002). Nerve growth factor expression and innervation of the painful intervertebral disc. J. Pathol. *197*, 286–292. https://doi.org/10.1002/path.1108.
18. Nerlich, A.G., Schaaf, R., Wälchli, B., and Boos, N. (2007). Temporo-spatial distribution of blood vessels in human lumbar intervertebral discs. Eur. Spine J. *16*, 547–555. https://doi.org/10.1007/s00586-006-0213-x.
19. Chandel, N.S. (2021). Glycolysis. Cold Spring Harbor Perspect. Biol. *13*, a040535. https://doi.org/10.1101/cshperspect.a040535.
20. Yu, J., Chai, P., Xie, M., Ge, S., Ruan, J., Fan, X., and Jia, R. (2021). Histone lactylation drives oncogenesis by facilitating m(6)a reader protein YTHDF2 expression in ocular melanoma. Genome Biol. *22*, 85. https://doi.org/10.1186/s13059-021-02308-z.
21. Meng, X., Baine, J.M., Yan, T., and Wang, S. (2021). Comprehensive Analysis of Lysine Lactylation in Rice (Oryza sativa) Grains. J. Agric. Food Chem. *69*, 8287–8297. https://doi.org/10.1021/acs.jafc.1c00760.
22. Song, Y., Liu, X., Stielow, J.B., de Hoog, S., and Li, R. (2022). Post-translational changes in Phialophora verrucosa via lysine lactylation during prolonged presence in a patient with a CARD9-related immune disorder. Front. Immunol. *13*, 966457. https://doi.org/10.3389/fimmu.2022.966457.
23. Fontana, G., See, E., and Pandit, A. (2015). Current trends in biologics delivery to restore intervertebral disc anabolism. Adv. Drug Deliv. Rev. *84*, 146–158. https://doi.org/10.1016/j.addr.2014.08.008.
24. Chacko, S.M., Ahmed, S., Selvendiran, K., Kuppusamy, M.L., Khan, M., and Kuppusamy, P. (2010). Hypoxic preconditioning induces the expression of prosurvival and proangiogenic markers in mesenchymal stem cells. Am. J. Physiol. Cell Physiol. *299*, C1562–C1570. https://doi.org/10.1152/ajpcell.00221.2010.
25. Li, W., Zhou, C., Yu, L., Hou, Z., Liu, H., Kong, L., Xu, Y., He, J., Lan, J., Ou, Q., et al. (2024). Tumor-derived lactate promotes resistance to bevacizumab treatment by facilitating autophagy enhancer protein RUBCNL expression through histone H3 lysine 18 lactylation (H3K18la) in colorectal cancer. Autophagy *20*, 114–130. https://doi.org/10.1080/15548627.2023.2249762.
26. Irizarry-Caro, R.A., Mcdaniel, M.M., Overcast, G.R., Jain, V.G., Troutman, T.D., and Pasare, C. (2020). TLR signaling adapter BCAP regulates inflammatory to reparatory macrophage transition by promoting histone lactylation. Proc. Natl. Acad. Sci. USA *117*, 30628–30638. https://doi.org/10.1073/pnas.2009778117.
27. Wang, Y., Li, H., Jiang, S., Fu, D., Lu, X., Lu, M., Li, Y., Luo, D., Wu, K., Xu, Y., et al. (2024). The glycolytic enzyme PFKFB3 drives kidney fibrosis through promoting histone lactylation-mediated NF-κB family activation. Kidney Int. *106*, 226–240. https://doi.org/10.1016/j.kint.2024.04.016.
28. Desgeorges, T., Galle, E., Zhang, J., von Meyenn, F., and De Bock, K. (2024). Histone lactylation in macrophages is predictive for gene expression changes during ischemia induced-muscle regeneration. Mol. Metab. *83*, 101923. https://doi.org/10.1016/j.molmet.2024.101923.
29. Holm, S., Maroudas, A., Urban, J.P., Selstam, G., and Nachemson, A. (1981). Nutrition of

the intervertebral disc: solute transport and metabolism. Connect. Tissue Res. *8*, 101–119. https://doi.org/10.3109/03008208109152130.

30. Mokhbi Soukane, D., Shirazi-Adl, A., and Urban, J.P.G. (2007). Computation of coupled diffusion of oxygen, glucose and lactic acid in an intervertebral disc. J. Biomech. *40*, 2645–2654. https://doi.org/10.1016/j.jbiomech.2007.01.003.
31. Shamsuddin, A.M., and Hogan, M.L. (1984). Large intestinal carcinogenesis. II. Histogenesis and unusual features of low-dose azoxymethane-induced carcinomas in F344 rats. J. Natl. Cancer Inst. *73*, 1297–1305.
32. Wang, X., Fan, W., Li, N., Ma, Y., Yao, M., Wang, G., He, S., Li, W., Tan, J., Lu, Q., and Hou, S. (2023). YY1 lactylation in microglia promotes angiogenesis through transcription activation-mediated upregulation of FGF2. Genome Biol. *24*, 87. https://doi.org/10.1186/s13059-023-02931-y.
33. Pope, S.D., and Medzhitov, R. (2018). Emerging Principles of Gene Expression Programs and their Regulation. Mol. Cell *71*, 389–397. https://doi.org/10.1016/j.molcel.2018.07.017.
34. Cramer, P. (2019). Organization and regulation of gene transcription. Nature *573*, 45–54. https://doi.org/10.1038/s41586-019-1517-4.
35. Lee, Y., and Rio, D.C. (2015). Mechanisms and Regulation of Alternative Pre-mRNA Splicing. Annu. Rev. Biochem. *84*, 291–323. https://doi.org/10.1146/annurev-biochem-060614-034316.
36. Baßler, J., and Hurt, E. (2019). Eukaryotic Ribosome Assembly. Annu. Rev. Biochem. *88*, 281–306. https://doi.org/10.1146/annurev-biochem-013118-110817.
37. Wilkinson, M.E., Charenton, C., and Nagai, K. (2020). RNA Splicing by the Spliceosome. Annu. Rev. Biochem. *89*, 359–388. https://doi.org/10.1146/annurev-biochem-091719-064225.
38. Yin, D., Jiang, N., Cheng, C., Sang, X., Feng, Y., Chen, R., and Chen, Q. (2023). Protein Lactylation and Metabolic Regulation of the Zoonotic Parasite Toxoplasma gondii. Dev. Reprod. Biol. *21*, 1163–1181. https://doi.org/10.1016/j.gpb.2022.09.010.
39. Bowman, J.C., Petrov, A.S., Frenkel-Pinter, M., Penev, P.I., and Williams, L.D. (2020). Root of the Tree: the Significance, Evolution, and Origins of the Ribosome. Chem. Rev. *120*, 4848–4878. https://doi.org/10.1021/acs.chemrev.9b00742.
40. Matera, A.G., and Wang, Z. (2014). A day in the life of the spliceosome. Nat. Rev. Mol. Cell Biol. *15*, 108–121. https://doi.org/10.1038/nrm3742.
41. Fang, S., Zeng, F., Chen, R., and Li, M. (2022). SIAH1 promotes senescence and apoptosis of nucleus pulposus cells to exacerbate disc degeneration through ubiquitinating XIAP. Tissue Cell *76*, 101820. https://doi.org/10.1016/j.tice.2022.101820.
42. Jiang, Z., Zhao, Q., Chen, L., Luo, Y., Shen, L., Cao, Z., and Wang, Q. (2022). UBR3 promotes inflammation and apoptosis via DUSP1/p38 pathway in the nucleus pulposus cells of patients with intervertebral disc degeneration. Hum. Cell *35*, 792–802. https://doi.org/10.1007/s13577-022-00693-6.
43. Popovic, D., Vucic, D., and Dikic, I. (2014). Ubiquitination in disease pathogenesis and treatment. Nat. Med. *20*, 1242–1253. https://doi.org/10.1038/nm.3739.
44. Sun, Z., Zhao, H., Liu, B., Gao, Y., Tang, W.H., Liu, Z.H., and Luo, Z.J. (2021). AF cell derived exosomes regulate endothelial cell migration and inflammation: Implications for vascularization in intervertebral disc degeneration. Life Sci. *265*, 118778. https://doi.org/10.1016/j.lfs.2020.118778.
45. Gupta, V., and Bamezai, R.N.K. (2010). Human pyruvate kinase M2: a multifunctional protein. Protein Sci. *19*, 2031–2044. https://doi.org/10.1002/pro.505.
46. Israelsen, W.J., Dayton, T.L., Davidson, S.M., Fiske, B.P., Hosios, A.M., Bellinger, G., Li, J., Yu, Y., Sasaki, M., Horner, J.W., et al. (2013). PKM2 isoform-specific deletion reveals a differential requirement for pyruvate kinase in tumor cells. Cell *155*, 397–409. https://doi.org/10.1016/j.cell.2013.09.025.
47. Otto, A.M. (2016). Warburg effect(s)-a biographical sketch of Otto Warburg and his impacts on tumor metabolism. Cancer Metab. *4*, 5. https://doi.org/10.1186/s40170-016-0145-9.
48. Korsunsky, I., Millard, N., Fan, J., Slowikowski, K., Zhang, F., Wei, K., Baglaenko, Y., Brenner, M., Loh, P.R., and Raychaudhuri, S. (2019). Fast, sensitive and accurate integration of single-cell data with Harmony. Nat. Methods *16*, 1289–1296. https://doi.org/10.1038/s41592-019-0619-0.
49. Gulati, G.S., Sikandar, S.S., Wesche, D.J., Manjunath, A., Bharadwaj, A., Berger, M.J., Ilagan, F., Kuo, A.H., Hsieh, R.W., Cai, S., et al. (2020). Single-cell transcriptional diversity is a hallmark of developmental potential. Science (New York, N.Y.) *367*, 405–411. https://doi.org/10.1126/science.aax0249.
50. Li, P., Che, X., Gao, Y., and Zhang, R. (2020). Proteomics and Bioinformatics Analysis of Cartilage in Post-Traumatic Osteoarthritis in a Mini-Pig Model of Anterior Cruciate Ligament Repair. Med. Sci. Monit. *26*, e920104. https://doi.org/10.12659/MSM.920104.
51. Vesztrocy, A.W., and Dessimoz, C. (2017). A Gene Ontology Tutorial in Python. Methods Mol. Biol. *1446*, 221–229.
52. Cheng, A., Grant, C.E., Noble, W.S., and Bailey, T.L. (2019). MoMo: discovery of statistically significant post-translational modification motifs. Bioinformatics *35*, 2774–2782. https://doi.org/10.1093/bioinformatics/bty1058.
53. Deng, J.L., Xu, Y.H., and Wang, G. (2019). Identification of Potential Crucial Genes and Key Pathways in Breast Cancer Using Bioinformatic Analysis. Front. Genet. *10*, 695. https://doi.org/10.3389/fgene.2019.00695.

STAR★METHODS

KEY RESOURCES TABLE

REAGENT or RESOURCE	SOURCE	IDENTIFIER
Antibodies		
L-Lactyl Lysine	PTM Bio Inc	Cat# PTM-1401RM
VEGFA	Abcam	Cat# ab46154
β-ACTIN	Proteintech	Cat# 66009-1-Ig
AGGRECAN	Proteintech	Cat# 13880-1-AP
MMP3	Proteintech	Cat# 66338-1-Ig
Collagen II	Proteintech	Cat# 28459-1-AP
Chemicals, peptides, and recombinant proteins		
0.25% Trypsin	Boster	PYG0068
Type II collagenase	Biofroxx	2275MG100
Protease inhibitors	Boster	AR1182-1
Phosphatase inhibitors	Boster	AR1183
Trichostatin A	MedChemExpress	Trichostatin A
Nicotinamide	Sigma-Aldrich	72340
Critical commercial assays		
BCA protein assay kit	Beyotime	P0012S
Deposited data		
Single-cell sequencing data	GEO database	GSE165722
Mass spectrometry protomics data	This paper	PRIDE database (PXD048244)
Software and algorithms		
GraphPad Prism 9	Software	V.9.0.0
R	Software	V.4.0.4
Seurat package	https://satijalab.org/seurat/	V.4.1.1
Harmony package	Software	V.0.1.0
CytoTRACE	https://cytotrace.stanford.edu	V.0.3.3
Monocle3	https://doi.org/10.1038/s41586-019-0969-x	V.1.2.9
gene set variation analysis	GSVA package	V.1.44.2
motif-X algorithm	MoMo analysis tools	V.5.5.5
STRING database	https://cn.string-db.org	V.11.0
Cytoscape software	Software	V.3.8.2
Molecular Complex Detection	plug-in of Cytoscape	

EXPERIMENTAL MODEL AND STUDY PARTICIPANT DETAILS

Cell culture

NPCs were isolated from the central NP tissues of IVDs in 8-week male Sprague-Dawley rats weighing 220 g. NP tissues were separated under hypoxic condition and then digested using 0.25% trypsin at 37°C for 30 minutes, followed by type II collagenase digestion at 37°C for 3 hours. The isolated cells were cultured in DMEM/F12 medium supplemented with 10% fetal bovine serum (Gibco) and 1% penicillin/streptomycin (Gibco) in 5% CO_2 incubator at 37°C. NPCs were divided into two groups: normoxia control group (NC, cultured in 21% O_2) and hypoxic group (HY, cultured in 1% O_2) for 24 hours and then were collected for further analysis.

All animal experiments were conformed to the Institutional Animal Care and Use Committee (IACUC) of the Second Affiliated Hospital of Soochow University, Jiangsu, China. The study complied with Animal Research: Reporting *in Vivo* Experiments (ARRIVE) guidelines to minimize the discomfort and pain of the animals.

METHOD DETAILS

Single-cell data analysis

Single-cell sequencing data was obtained from GEO database (GSE165722), and the Seurat package (version 4.1.1, https://satijalab.org/seurat/) on R (version 4.0.4) was used for cell normalization, dimension-reduction, clustering and differentially expressed gene analysis. Harmony package (version 0.1.0) was used to correct the batch effect.[48] RunHarmony (group.by.vars = "orig.ident", reduction = "pca",dims.use = NULL,theta = NULL,lambda = NULL,sigma = 0.1,max.iter.harmony = 10,max.iter.cluster = 20,assay.use = "RNA"). CytoTRACE analysis was applied for cell stem stage analysis with default parameter.[49] iCytoTRACE(enableFast = TRUE, ncores = 8, subsamplesize = 1000). Monocle3 (version 1.2.9) package (https://doi.org/10.1038/s41586-019-0969-x) was applied to construct single-cell pseudo-time trajectories. We applied the gene set variation analysis (GSVA) method to assign pathway activity estimates for individual NPC, as implemented in the GSVA package (version 1.44.2).

Western blotting analysis

NPCs were homogenized in RIPA buffer containing 1% phosphatase and protease inhibitors, 3μM Trichostatin A (MedChemExpress) and 50mM Nicotinamide (Sigma-Aldrich). After centrifugated at 12,000 rpm for 20 minutes at 4°C, protein was collected. Then BCA protein assay kit (Beyotime) was used to detect protein concentration. Protein samples were separated by sodium dodecyl sulfate the polyacrylamide gel electrophoresis (SDS-PAGE) and electro-transferred to 0.45μm PVDF membrane (Millipore), blocked with 5% BSA for 1 hour. Next, the membranes were incubated with primary antibodies including AGGRECAN (Proteintech, 1:1000), MMP3 (Proteintech, 1:1000), SOX9 (CST, 1:1000), L-Lactyl Lysine (PTM Bio lnc, 1:1000), VEGFA (Abcam, 1:1000), β-ACTIN (Proteintech, 1:5000) overnight at 4°C. After washing with TBST for three times, the membranes were then immunoblotted with corresponding secondary antibodies and visualized with the SuperSignal West Pico chemiluminescent substrate (Thermo Fisher Scientific).

Proteomic analysis

NPCs were sonicated three times on ice with high intensity ultrasonic processor (Scientz) in lysis buffer (8 M urea, 1% protease inhibitor cocktail, 3 μM TSA and 50 mM NAM). The remaining debris was removed by centrifugation at 12,000 g for 10 minutes. The supernatant was collected and protein concentration was determined with BCA kit. And for digestion, the protein solution was reduced with 5 mM dithiothreitol for 30 minutes at 56°C and alkylated with 11 mM iodoacetamide for 15 minutes at room temperature in darkness. The protein samples were then diluted with 100 mM TEAB to urea concentration less than 2 M. Finally, trypsin was applied at 1:50 trypsin-to-protein mass ratio for the first digestion overnight and 1:100 trypsin-to-protein mass ratio for second 4 hours digestion. Finally, the peptides were desalted by C18 SPE column. There are three samples in each group.

To enrich modified Kla peptides, tryptic peptides dissolved in NETN buffer (100 mM NaCl, 1 mM EDTA, 50 mM Tris-HCl, 0.5% NP-40, pH 8.0) were incubated with pre-washed antibody beads (PTM Bio lnc) at 4°C overnight with gentle shaking. Then the beads were washed four times with NETN buffer and twice with H_2O. The bound peptides were eluted from the beads with 0.1% trifluoroacetic acid. Finally, the eluted fractions were combined and vacuum-dried. For liquid chromatography-tandem mass spectrometry (LC-MS/MS) analysis, the resulting peptides were desalted with C18 ZipTips (Millipore) according to the manufacturer's instructions. Finally, the peptides were subjected to capillary source followed by the timsTOF Pro (Bruker Daltonics) mass spectrometry. The electrospray voltage applied was 1.60 kV. Precursors and fragments were analyzed at the TOF detector, with a MS/MS scan range from 100 to 1700 m/z. The timsTOF Pro was operated in parallel accumulation serial fragmentation (PASEF) mode. Precursors with charge states 0 to 5 were selected for fragmentation, and 10 PASEF-MS/MS scans were acquired per cycle. The dynamic exclusion was set to 30 seconds.

The resulting MS/MS data were processed using MaxQuant search engine (version 1.6.15.0). Tandem mass spectra were searched against the human SwissProt database (20422 entries) concatenated with reverse decoy database.

Bioinformatics analysis

Clustering analysis was used to classify the similarity of the data. The hierarchical clustering K-mean algorithm was applied to distinguish data with high similarity and low similarity, and the two dimensions of samples and variables were considered at the same time.[50] Gene Ontology (GO), a major bioinformatics initiative, was used to define the representation of gene and gene product properties across all species.[51] The results of GO function analysis, which was based on the function entry for the unit, immediately displayed the general enrichment characteristics of the differentially expressed proteins that were enriched in the GO function. The Kyoto Encyclopedia of Genes and Genomes (KEGG) was consulted for its route data on metabolic, genetic and environmental data processing, cellular functions, biological systems, human illnesses, and medication development. The systematic and comprehensive understanding of NPCs biological processes were analyzed by KEGG. The detected total protein and KEGG pathway analysis were handled as a single entity. The target protein sets were annotated using the KEGG automated annotation server tool program (KASS).

Motif analysis

Based on motif-X algorithm, MoMo analysis tools (for Modification Motifs) was used to detect amino acid sequence around protein PTM motifs.[52] All identified peptide sequences containing 10 amino acids upstream and downstream of the lactylation site were used as analysis objects. The number of peptides in a characteristic sequence form is more than 20 and the P value of statistical test is less than 0.000001 which is

considered to be a motif modifying the peptide. Based on the results of MoMo analysis, heat map was used to show the degree of frequency change (DS) of amino acids near the modification site. DS was calculated as the following equation:

$$DS = -Log10\ (p.\ value) * sign\ (diff.\ percent)$$

Protein-protein interaction network

The STRING database (version 11.0) is used to build protein-protein interaction (PPI) network of differentially expressed proteins to examine the functional connections between proteins.[53] STRING defines a metric called "confidence score" to estimate interaction confidence and we fetched interaction protein with confidence score $\geq$ 0.7 (high confidence). Next, interaction network form STRING was visualized in Cytoscape software. Besides, the Molecular Complex Detection (MCODE) plug-in of Cytoscape software was used to investigate the important modules in the PPI network. The advanced options set as degree cutoff = 2, Node Score cutoff = 0.2 and K-Core = 2.

Tube formation assay

Conditioned medium collected from NPCs cultured in different oxygen environment for 24 hours. Growth factor-reduced Matrigel matrix (10 mg/mL) was added to 96-well plate with 50 μl per well, and then incubated at 37°C for 30 minutes to allow for solidification. Subsequently, endothelial progenitor cells (EPCs) were seeded onto the Matrigel-coated surfaces at a density of 1.0×10^4 cells per well. EPCs were cultured with the conditioned medium and finally stained with Calcein-AM.

QUANTIFICATION AND STATISTICAL ANALYSIS

The quantification and statistical analysis were conducted using the GraphPad Prism 9. To compare the means or data distribution of continuous variables, the unpaired 2-tailed Student t-test was used. For GO/KEGG enrichment analysis, Fisher's exact test was used. When $P<0.05$, difference was deemed statistically significant.